

Radical-Cationic Gaseous Amino Acids: A Theoretical Study

Kailee N. Sutherland, Philippe C. Mineau, and Galina Orlova*

Department of Chemistry, St. Francis Xavier University, Nova Scotia, Canada, B2G 2W5

Received: February 11, 2007; In Final Form: May 20, 2007

Three major forms of gaseous radical-cationic amino acids (RCAAs), keto (COOH), enolic (C(OH)OH), and zwitterionic (COO⁻), as well as their tautomers, are examined for aliphatic Ala^{•+}, Pro^{•+}, and Ser^{•+}, sulfur-containing Cys^{•+}, aromatic Trp^{•+}, Tyr^{•+}, and Phe^{•+}, and basic His^{•+}. The hybrid B3LYP exchange-correlation functional with various basis sets along with the highly correlated CCSD(T) method is used. For all RCAAs considered, the main stabilizing factor is spin delocalization; for His^{•+}, protonation of the basic side chain is equally important. Minor stabilizing factors are hydrogen bonding and 3e–2c interactions. An efficient spin delocalization along the N–C_α–C(O–)O moiety occurs upon H-transfer from C_α to the carboxylic group to yield the captodative enolic form, which is the lowest-energy isomer for Ala^{•+}, Pro^{•+}, Ser^{•+}, Cys^{•+}, Tyr^{•+}, and Phe^{•+}. This H-transfer occurs in a single step as a 1,3-shift through the σ -system. For His^{•+}, the lowest-energy isomer is formed upon H-transfer from C_α to the basic side chain, which results in a keto form, with spin delocalized along the N–C_α–C=O fragment. Trp^{•+} is the only RCAA that favors spin delocalization over an aromatic system given the low ionization energy of indole. The lowest-energy isomer of Trp^{•+} is a keto form, with no H-transfer.

Introduction

The chemistry of radical-cationic amino acids (RCAAs) and polypeptides has received significant attention^{1–16} particularly after the discovery by the Siu group^{1,2} that gaseous RCAAs can be readily formed in a mass spectrometer. The new method is based on the low-energy collision-induced electron-transfer dissociation of [Cu(II)(L)(M)]²⁺ complexes, where L is an auxiliary ligand and M is a polypeptide or an amino acid. Upon dissociation, an electron transfers from M to the copper center to yield [Cu(I)(L)]⁺ and M^{•+}; the latter undergoes further fragmentations.^{1–12} The new technique is particularly important for structural determination of polypeptides since the fragmentation of radical cations^{1–12} is different from that of protonated species, which are typically used in mass spectrometry.

The [Cu(II)(L)(M)]²⁺ complexes mimic type 1 copper sites, which are present in cupredoxins, a family of electron-transfer proteins.¹⁷ The electron-transfer dissociation of [Cu(II)(L)(M)]²⁺ might serve as a gaseous model of redox reactions in living cells, responsible for many physiological disorders. In particular, oxidation at sulfur in the methionine (Met) residue by Cu(II) yields a radical cation and initiates a sequence of chemical reactions leading to disease development such as glaucoma¹⁸ and Alzheimer's disease.¹⁹ A systematic theoretical study on the redox chemistry of methionine-containing systems related to Alzheimer's disease was conducted by the Rauk group.¹³

Another important aspect of RCAA chemistry arose with the gaseous synthesis of Gly^{•+} and Ala^{•+} from radical-cationic hydroxylamine and the corresponding carboxylic acids, successfully performed by the Bohme group.¹⁴ This experiment combined with a theoretical study^{14b} proves that the formation of amino acids from small organic molecules and ions (radical cations) is possible in the interstellar media. Gly, Ala, and

γ -aminobutyric acid have been detected in carbonaceous chondrite meteorites.²⁰ Several authors have made a suggestion that amino acids of chondrite meteorites were formed abiotically in interstellar media and delivered to the early Earth.^{21,22}

Success in the abovementioned research areas demands understanding of the trends in the formation, stabilities, and rearrangements of RCAAs, which determine their chemistry. Here we apply hybrid density functional theory (DFT) in order to study the major isomers of radical-cationic alanine, proline, serine, cysteine, tryptophan, tyrosine, phenylalanine, and histidine. Ala represents a parent amino acid, Pro is unique due to its secondary amino group, and Ser and Cys contain hetero atoms, oxygen and sulfur in their side chains. Trp, Tyr, and Phe are aromatic amino acids, while His combines some aromatic and strong basic properties. Another object of this paper is to determine the origin and mechanisms of proton migrations in RCAAs, which proved to be different from those in protonated amino acids.⁵

Methods

Density functional theory was employed to determine geometries, energetics, and Mulliken atomic spin densities using the Gaussian 03 package.²³ The B3LYP exchange-correlation functional, with Becke's three-parameter hybrid exchange, B3,²⁴ and the correlation functional by Lee, Yang and Parr, LYP,²⁵ was used. A moderate double- ζ 6-31+G(d) basis set was predominantly employed. Several larger basis sets, 6-31++G(d,p), 6-311+G(d), 6-311+G(d,p), 6-311++G(d,p), and 6-311++G(df,p), were also used to verify the reliability of 6-31+G(d). For all the RCAAs considered, B3LYP shows essentially no dependence on an increase in the size and flexibility of the basis set. In most cases, an increase in the basis set caused an increase in the energy gaps between the RCAA isomers and reaction profiles; no changes in the ordering of the isomers were obtained. Excellent performance of B3LYP with the moderate basis sets in predictions of RCAAs has been

* Corresponding author. Phone: (902) 867-5237. Fax: (902) 867-2414. E-mail: gorlova@stfx.ca.

proven in a number of publications.^{5,12,13,16a,e} The drawback of B3LYP in predictions on Gly⁺, Ala⁺, and Ser⁺ has also been reported.^{16c,g} The B3LYP exchange-correlation functional overestimates the stability of the conformers with the amino group in the cis position to the carboxyl oxygen and places the cis conformers slightly (ca. 2 kcal/mol) below the conformers with the NH₂ and OH groups in the trans position. The MP2 and CCSD(T) methods change the ordering in favor (ca. 2 kcal/mol) of the trans conformers. This drawback of B3LYP has been analyzed and attributed to the self-interaction error. However, the reaction barriers predicted with B3LYP are in a good accord with the CCSD(T) results.^{16c,g} Since the energy difference between the two conformers and the rotational barrier are small, this drawback of B3LYP does not affect the general trends studied in this paper.

The trends in geometries and energetics predicted with the B3LYP/6-31+G(d) method in the present work are applicable for large radical-cationic biosystems, which are currently under active investigation in our group. Thus, the B3LYP/6-31+G(d) values are predominantly reported (except in cases specially mentioned). For selected structures on the competitive reaction pathways, single-point energy calculations were performed with the coupled-cluster method, CCSD(T),²⁶ and the 6-311++G(d,p) basis set using the B3LYP/6-311++G(d,p) geometries and zero-point vibrational energy corrections.

For all RCAAs, harmonic vibrational frequencies were computed to verify minima (all real frequencies) and transition state structures (one imaginary frequency). The connections between transition states and adjacent minima on the potential energy surfaces were verified using the intrinsic reaction coordinate technique (IRC) developed by Gonzalez and Schlegel.^{27,28} All relative energies include zero-point vibrational energy (ZPVE) corrections. For reaction profiles, the relative Gibbs energies at 298 K are also reported. Molecular (Kohn-Sham) orbitals were constructed using the GaussView software package.²⁹

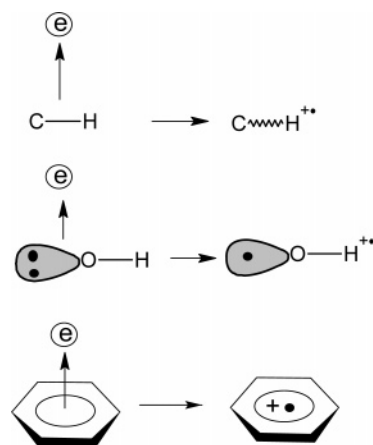
In order to locate the lowest-energy conformers, the systematic conformation search function of Spartan06³⁰ was used at the HF/3-21G level of theory, followed by visual inspection and DFT calculations.

Results and Discussion

1. Keto, Enolic, and Zwitterionic Forms of RCAAs. A radical cation of an amino acid can be formed by removing an electron from the closed-shell system; thus, amino acids with low ionization energies (IEs) should readily form radical cations. Although the experimental values of IE are known only for a few gaseous amino acids, one might propose that the aromatic and sulfur-containing amino acids should have the lowest IEs. Ionization may cause significant changes in the geometries and energetics of an amino acid since the covalent bonds, in general, become weaker. This is supported by the following experimental observations: the cleavage of a C_α-C_β bond resulting in the loss of the side chain and the C_β proton migrations (i.e., a C_β-H bond cleavage) are low-energy processes, which occur readily upon collision-induced dissociations of radical-cationic polypeptides and do not have analogues in protonated peptides.⁵

Ionization may also cause the appearance of a new type of bonding: a three-electron, two-center, 3e-2c, interaction discovered for Met⁺ by the Rauk group.^{13a} Although the 3e-2c bonding is weaker than a typical 2e-2c covalent bond, it is crucial for the stabilization of Met⁺^{13a} and significant for Cys⁺.^{16c} Another possible stabilizing factor for RCAAs is intramolecular hydrogen bonding, which is particularly impor-

SCHEME 1



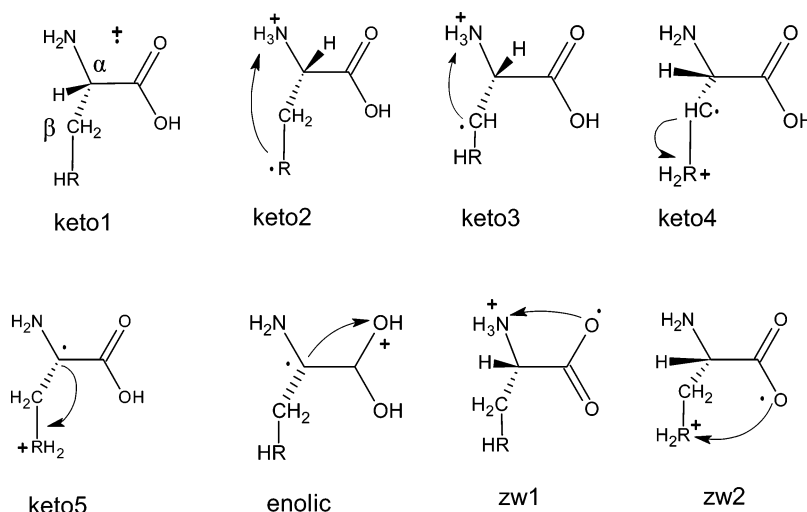
tant for the amino acids containing proton donors (Ser, Cys) and proton acceptors (His) in the side chains.

Mechanistically, an electron can be removed from a covalent bond, from a lone pair of a heteroatom (O, N, S), or from the π -system of an aromatic ring as shown in Scheme 1. The former process results in a strong polarization of the bond and has the greatest effect on the resulting radical-cationic structure. Ionization from a lone pair, which might be favorable for the amino acids containing sulfur (e.g., Cys) and secondary amines (e.g., Pro), causes a moderate polarization of the bond. Ionization from the π -system of an aromatic ring should have a small structural effect since an unpaired electron and a hole can be effectively delocalized over a conjugated system. Thus, one could anticipate significant changes in the structures of the aliphatic amino acids and minor changes for the aromatic ones. This mechanistic approach is consistent with the following experimental observations: the aromatic amino acids with the lowest IEs (Trp and Tyr) readily form radical cations, M⁺, upon electron-transfer dissociation of the [Cu(II)(L)(M)]²⁺ complexes, suppressing a competitive proton-transfer dissociation, which yields protonated amino acids, MH⁺.^{1,2,5} In contrast, Cu(II) complexes with the aliphatic amino acids undergo predominantly proton-transfer dissociation and demand a very thorough selection¹¹ of an auxiliary ligand, L, in order to facilitate the electron-transfer dissociation.

A gaseous RCAA may exist in three major forms based on the structure of the carboxylic group: keto (COOH), enolic (C(OH)OH), and zwitterionic (COO⁻), shown in Chart 1. Each form, in turn, may have several low-energy isomers, based on the origin and/or destination of the hydrogen being transferred, as shown with the arrows in Chart 1. The keto1 isomer is formed by ionization of a low-energy conformer of the molecular form of a neutral gaseous amino acid, with no H-transfer. The keto2 isomer is due to H-transfer from the protic side chain, RH (e.g., Ser, Cys), to the amino group. The keto3 isomer is formed upon H-transfer from the C_β to the amino group that should be anticipated for the aromatic amino acids (Trp, Tyr, Phe, His).⁵ The keto4 and keto5 isomers are formed upon H-transfer to the basic group of the side chain from the C_β and C_α, respectively.

The enolic form is formed upon H-transfer from the C_α to the carboxylic group. It has been previously shown by Simon, Sodupe, and Bertran^{16a} that the enolic form is the lowest-energy isomer for Gly⁺. The zwitterionic forms occur upon H-migration from the carboxylic group to either the amino group (zw1) or the basic side chain (zw2). Although neutral gaseous amino acids do not exist as zwitterions, the presence of a net charge makes a charge-separated form thermodynamically

CHART 1



stable.¹⁵ Rodríguez-Santiago et al.^{16g} have shown that a zwitterionic form corresponds to a local minimum on the potential energy surface (PES) of Gly^{•+}. All the major isomers of RCAAs are connected on the PES via proton migrations.

2. Aliphatic Amino Acids: Ala^{•+}, Pro^{•+}, Ser^{•+}, Cys^{•+}. (a) Ala^{•+}. The lowest-energy conformers for the enolic, keto1, and zw1 forms of Ala^{•+} are reported in Figure 1 along with selected geometries and relative energetics.

The Ala^{•+}-enolic isomer is formed by H-transfer from the C_α to the carbonyl oxygen; this is the lowest-energy isomer of Ala^{•+}. Ala^{•+}-keto1 is 21.6 kcal/mol higher in energy than the enolic form and features an elongated C_α-C_{carboxylic} bond (1.620 Å) aligned with the lone pair of the nitrogen atom and a shortened C-N bond (1.402 Å). The zwitterionic isomer, Ala^{•+}-zw1, is formed by H-transfer from the carboxylic group to the amino group and corresponds to a local minimum, which is 32.3 kcal/mol above the enolic form.

A Mulliken analysis of the atomic spin densities reveals that, for the lowest-energy enolic form, an unpaired electron is

delocalized along the main chain providing significant stabilization. For organic radicals, this effect is known as *captodative*^{31a} stabilization, which is observed when an unpaired electron resides between a π-donor (the N atom of the amino group) and a π-acceptor (the carbonyl group).^{31b} For Ala^{•+}-enolic, the C_α-C_{carboxylic} bond is shortened (1.411 Å); the singly occupied molecular orbital (SOMO) reported in Figure 1 indicates π-bonding for the C_α-C_{carboxylic} fragment. In contrast, for the high-energy isomers, spin is localized. For the keto1 form, the unpaired electron resides essentially on the nitrogen atom (0.7e) and on the carbonyl oxygen atom (0.2e). For the zw1 form, spin is localized on the oxygen atom, which is in the trans position to the amino group (0.7e) and on the cis oxygen atom (0.3e). Formally, the zwitterionic form can be classified as a *distonic*^{31c} radical cation, with separated spin (the carboxylate group) and charge (the protonated amino group) sites. However, this separation is not really stabilizing since it is not associated with delocalization of an unpaired electron.

Mechanistically, ionization of a neutral gaseous Ala can be considered as a removal of an electron from the C_α-C_{carboxylic} bond. The resulting structure, Ala^{•+}-keto1, can be stabilized by H-transfer from the C_α to the carbonyl oxygen: the carboxylic group acts as a base while C_α-H acts as an acid. The acidity of the methylene group in RCAAs has the same nature as the acidity of CH₄^{•+}, which has been studied by Gil, Bertran, and Sodupe.^{16b}

(b) Pro^{•+}. The lowest-energy conformers for the enolic, keto1, and zw1 forms of Pro^{•+} are shown in Figure 2. Similar to Ala^{•+}, the lowest-energy isomer of Pro^{•+} is enolic, followed by the keto1 and zw1 forms. However, the energy gap between Pro^{•+}-enolic and Pro^{•+}-keto1 is notably smaller (12.8 kcal/mol for Pro^{•+} versus 28.1 kcal/mol for Ala^{•+}). Analyses of geometries and Mulliken spin densities reveal the nature of this difference. Pro^{•+}-enolic is captodative and has a shortened C_α-C_{carboxylic} bond, as in the case of Ala^{•+}. The keto1 form of Pro^{•+} has spin localized on the nitrogen atom (0.9e) and all the typical covalent bond lengths, in contrast to Ala^{•+}-keto1. Mechanistically, ionization from the lone pair of the N atom of the secondary amino group, with relatively low IE, is more favorable than ionization from the covalent α-C-C_{carboxylic} bond as in the case of Ala^{•+}. Spin localization on the carboxylate group is not favorable: the zwitterionic form, Pro^{•+}-zw1, is a high-energy local minimum, which is 30.4 kcal/mol above Pro^{•+}-enolic, similar to that for Ala^{•+}.

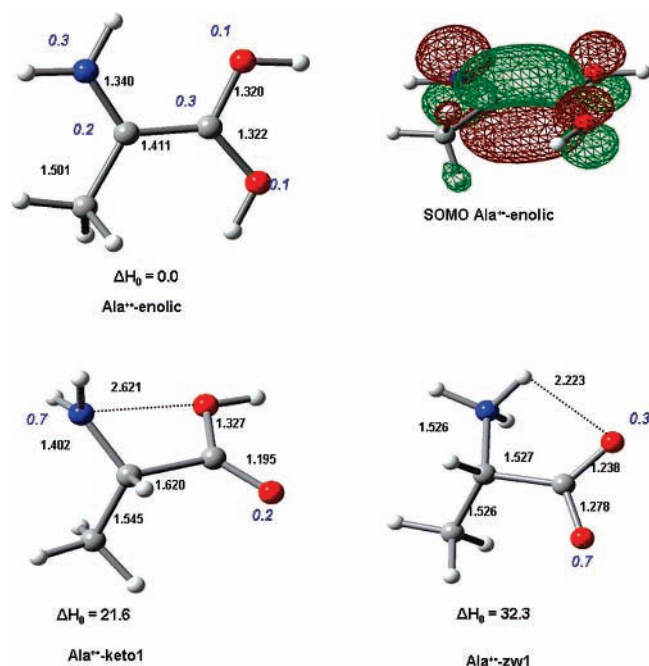


Figure 1. Lowest-energy conformers of three major isomers of Ala^{•+} predicted with the B3LYP/6-31+G(d) method. Selected geometries are in Å. Relative enthalpies at 0 K are in kcal/mol. Mulliken spin densities are in blue italics. SOMO for Ala^{•+}-enolic is sketched.

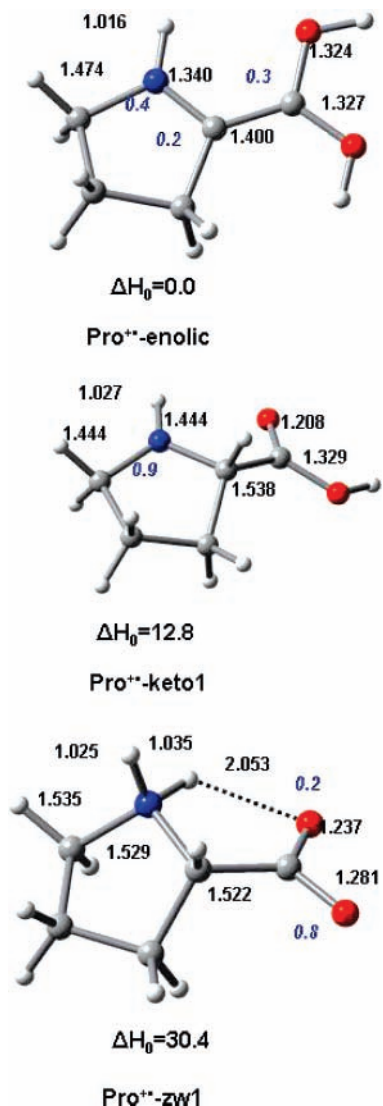


Figure 2. Lowest-energy conformers of three major isomers of Pro⁺ predicted with the B3LYP/6-31+G(d) method. Selected geometries are in Å. Relative enthalpies at 0 K are in kcal/mol. Mulliken spin densities are in blue italics.

(c) Ser⁺. The side chain of Ser⁺ contains the hydroxyl group, which might form a hydrogen bond or donate a proton to the amino group; the latter results in the keto2 form. The lowest-energy conformers of Ser⁺-enolic, Ser⁺-keto1, Ser⁺-keto2, and Ser⁺-zw1 isomers are shown in Figure 3. Similar to the enolic forms of Ala⁺ and Pro⁺, Ser⁺-enolic is the lowest-energy isomer, with an unpaired electron delocalized along the main chain, which appears to be a major stabilizing factor for RCAAs. The new stabilizing factor, which appears in Ser⁺-enolic, is the H-O[•]⋯H-O hydrogen bonding between the side chain and the protonated carboxylic group.

Ser⁺-keto1 is 22.8 kcal/mol higher in energy than the enolic form. For this isomer, the C_α-C_β bond is significantly elongated (1.797 Å); an unpaired electron is distributed equally between the weakly bound fragments. H-transfer from the side-chain carboxyl to the amino group yields Ser⁺-keto2, which is 23.3 kcal/mol above the enolic isomer. For Ser⁺-keto2, an unpaired electron resides entirely on the oxygen atom of the side chain that apparently is not energetically favorable. Even less favorable is spin localization on the carboxylate group for the zwitterionic form, Ser⁺-zw1, which is 33.2 kcal/mol higher in energy than Ser⁺-enolic.

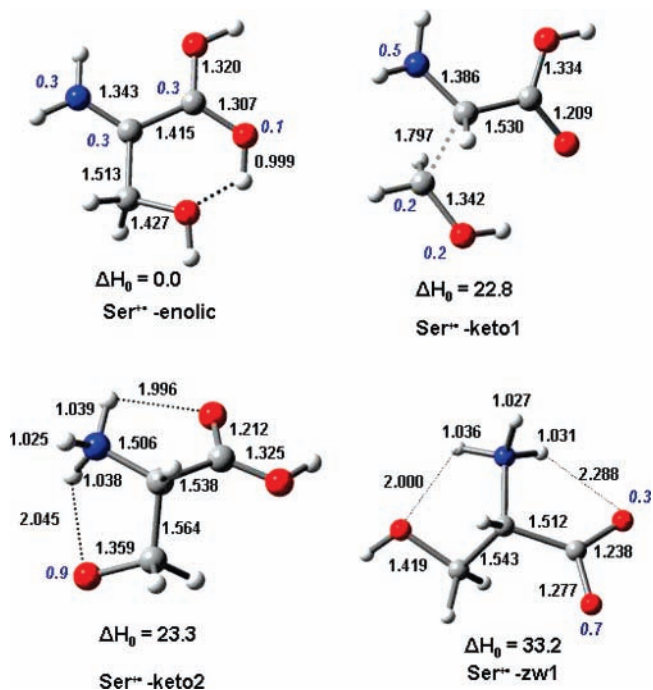


Figure 3. Lowest-energy conformers for major isomers of Ser⁺ predicted with the B3LYP/6-31+G(d) method. Selected geometries are in Å. Relative enthalpies at 0 K are in kcal/mol. Mulliken spin densities are in blue italics.

Mechanistically, ionization of a neutral Ser occurs from the covalent bonds rather than from the lone pair of the oxygen atoms of the carboxyl or hydroxyl groups. An additional H-bonding in the keto2 and zwitterionic forms does not compete with the captodative stabilization in the enolic form. The N-H[•]⋯O[•] and O-H[•]⋯O[•] hydrogen bonds of Ser⁺-keto2 and Ser⁺-zw1 contain only slightly elongated N-H and O-H bonds (Figure 3), since O[•] is a poorer base than the carbonyl oxygen in closed-shell compounds. Assuming that the strength of an A-H[•]⋯B intramolecular hydrogen bond increases with an increase in the A-H distance,³² the N-H[•]⋯O[•] and O-H[•]⋯O[•] interactions are rather weak.

(d) Cys⁺. Cys is a sulfur analogue of Ser. Cys⁺ forms the same four types of low-energy isomers as Ser⁺, but the presence of a period 3 element in the side chain affects the relative energetics and electronic structure dramatically. The lowest-energy conformers for the Cys⁺-enolic, Cys⁺-keto1, Cys⁺-keto2, and Cys⁺-zw1 isomers of Cys⁺ are shown in Figure 4. In sharp contrast to Ser⁺-keto1, the lowest-energy conformer of Cys⁺-keto1 has no elongated bonds. A new type of stabilization appears: a 3e-2c interaction between the sulfur and nitrogen atoms, with spin densities of 0.6e and 0.4e, respectively. Cys⁺-keto1 is also stabilized by N-H[•]⋯O hydrogen bonding. The Cys⁺-keto2 isomer, with hydrogen transferred from the SH group to the amino group, is notably lower in energy than Cys-keto1 (by 11.9 kcal/mol), in contrast to the corresponding isomers of Ser⁺. For Cys⁺-keto2, the localization of an unpaired electron on the sulfur atom is energetically favorable given the low IE of a period 3 element. The Cys⁺-keto2 isomer is also stabilized by the N-H[•]⋯S and N-H[•]⋯O hydrogen bonds. The enolic form, Cys⁺-enolic, is the lowest-energy isomer, similar to that for Ala⁺, Pro⁺, and Ser⁺, albeit the energy gaps between the keto forms and enolic form are small.

Stabilization of the Cys⁺-enolic form is caused by spin delocalization and by the O-H[•]⋯S and N-H[•]⋯O hydrogen

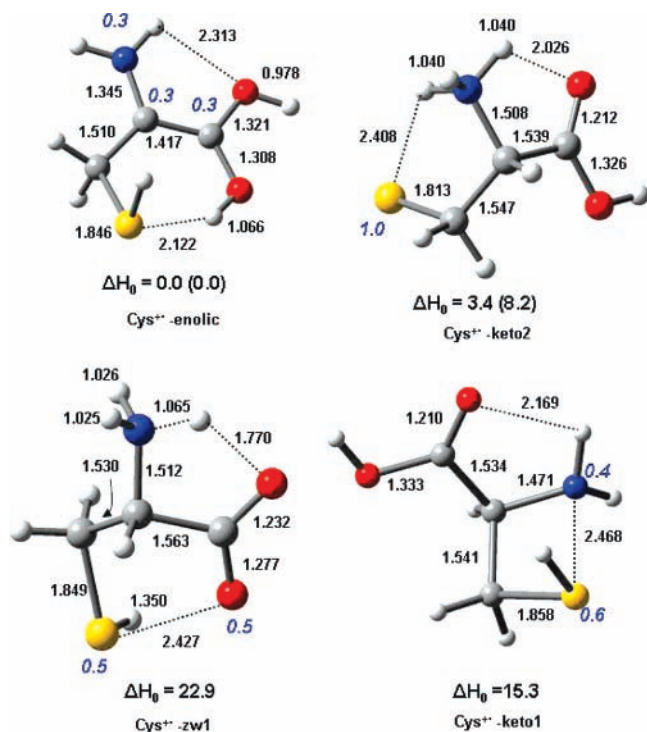


Figure 4. Lowest-energy conformers for the major isomers of Cys*⁺ predicted with the B3LYP/6-31+G(d) method. Selected geometries are in Å. Relative enthalpies are in kcal/mol; values in parentheses are from B3LYP/6-311++G(df,p). Mulliken spin densities are in blue italics.

bonds. Cys*⁺-zw1, which is formed by H-transfer from the carboxylic group to the amino group, is also slightly lower in energy than the zwitterionic structures of other aliphatic RCAAs, with an energy gap between Cys*⁺-enolic and Cys*⁺-zw1 of 22.8 kcal/mol. Cys*⁺-zw1 is stabilized by the N–H···O hydrogen bonding and by the S···O 3e–2c interaction, with the spin equally distributed between the S and O atoms. This is in contrast to the spin density distribution in Ala*⁺-zw1, Pro*⁺-zw1, and Ser*⁺-zw1, where an unpaired electron resides entirely on the carboxylate group. Since the O atom involved in the N–H···O bonding in Cys*⁺-zw1 has a zero Mulliken spin density, the N–H bond is longer than in the case of Ser*⁺-zw1 (1.065 and 1.031 Å, respectively).

Mechanistically, ionization of a neutral gaseous Cys occurs from the lone pair of the S atom rather than from the C–C covalent bond as in the case of Ala and Ser. Spin delocalization along the main chain in the Cys*⁺-enolic isomer is still more favorable than its localization on the sulfur atom in Cys*⁺-keto2, yet the energy gap between these isomers, as calculated with the B3LYP/6-31+G(d) and B3LYP/6-311++G(df,p) methods, is only 3.4 and 8.2 kcal/mol, respectively. An unpaired electron on the sulfur site can be stabilized with the methyl group: for Met*⁺, the keto-1 form is the global minimum on PES.^{13a}

3. Migrations of H_{Cα}: the π - and σ -Type Mechanisms. The lowest-energy enolic isomers of Ala*⁺, Pro*⁺, Ser*⁺, and Cys*⁺ are formed upon proton migration from the C_α to the carbonyl oxygen. The H_{Cα}-transfer may occur through the π -system and through the σ -system of RCAA. The potential energy profiles for two possible mechanisms and the SOMOs for the transition state structures predicted for Gly*⁺ are shown in Figure 5. When the π -system is involved, hydrogen can migrate above the planar structure of [Gly–H]⁺ from the C_α to the carbonyl oxygen. Since the p _{π} -atomic orbitals (AOs) of the C_α and carbonyl oxygen do not overlap (see the SOMOs in Figure 5), there cannot be a

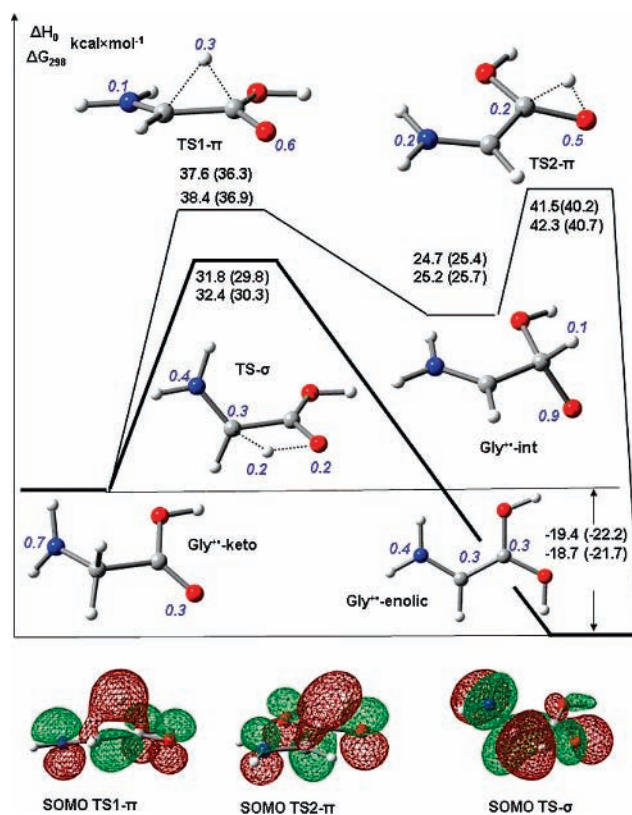


Figure 5. The σ -type and π -type mechanisms of H_{Cα}-transfer for the keto–enolic rearrangement of Gly*⁺ predicted with the B3LYP/6-31+G(d) and B3LYP/6-311++G(d,p) (values in parentheses) methods. The ΔH_0 values are on top, ΔG_{298} values on bottom. SOMOs for transition structures are sketched. Mulliken spin densities are in blue italics.

direct 1,3-shift through the π -system. Indeed, the π -type transfer occurs via a stepwise mechanism as a sequence of two 1,2-shifts. The first 1,2-shift is from the C_α to the carbon atom of the carboxylic group, via a transition state structure, TS1- π , with a reaction barrier of 37.6 kcal/mol. The TS1- π leads to an intermediate, Gly*⁺-int, which is 24.7 kcal/mol above the Gly*⁺-keto1 isomer. The second step of the π -type H-transfer is a 1,2-shift from the carboxylic carbon to the carbonyl oxygen, via a transition state, TS2- π , and a reaction barrier of 41.5 kcal/mol. This is the rate-determining step on the π -type reaction pathway.

When the σ -system is involved, hydrogen migrates in the H–C_α–C=O plane. Since the σ -AOs of C_α–H and the carbonyl oxygen overlap (see the SOMO in Figure 5), direct transfer is possible. Indeed, σ -type H-transfer occurs via a concerted mechanism as a 1,3-shift in the H–C_α–C=O plane. The corresponding transition state, TS- σ , is 5.6 and 9.7 kcal/mol lower in energy than TS1- π and TS2- π , respectively, as predicted with the B3LYP/6-31+G(d) method. These values increase to 6.5 and 10.4 kcal/mol, respectively, with an increase in the basis set to 6-311++G(d,p). The two types of proton transfer are reminiscent of the σ - and π -type hydrolyses of radical-cationic ketene to form acetic acid; a σ -type hydrolysis only yields the product.^{14b} This selectivity reflects the dual nature of a radical cation which may act as a cation, through the σ -system, and as a radical, through the π -system.

The σ -type concerted H-transfer is competitive with another stepwise mechanism, which has been earlier proposed for the keto–enolic rearrangement of Gly*⁺.^{16a} This rearrangement occurs via a 1,2 H-shift from the C_α to the amino group (C_α → NH₂) through the π -system, which yields a low-energy inter-

mediate, $\text{NH}_3\text{C(H)COOH}^+$. This is the rate-determining step. The second step involves a low-barrier 1,4 H-shift from NH_3 to the carboxylic group through the σ -system to yield $\text{Gly}^{\bullet+}$ -enolic. The corresponding reaction profile is reported in the Supporting Information (Figure S1). It has been shown at the CCSD(T) level of theory that the barrier to the $\text{C}_\alpha \rightarrow \text{NH}_2$ shift is ca. 5 kcal/mol lower than the barrier to the 1,2-shift from the carboxylic carbon to the carbonyl oxygen.^{16a} Thus, for the keto-enolic rearrangement the stepwise H-transfer via the NH_2 group is energetically more favorable than the stepwise H-transfer via the C atom of the carboxylic group. However, the concerted 1,3 H-shift is the most favorable. Our calculations show that the transition state for the $\text{C}_\alpha \rightarrow \text{NH}_2$ shift is higher in energy than the TS- σ by 7.8, 8.2, and 5.1 kcal/mol as predicted with the B3LYP/6-31+G(d), B3LYP/6-311++G(d,p), and CCSD(T)/6-311++G(d,p)//B3LYP/6-311++G(d,p) methods, respectively (Table S1).

The reaction barriers to the concerted and stepwise keto-enolic rearrangements for other aliphatic RCAAs apparently are lower in energy than those for $\text{Gly}^{\bullet+}$, since the side chain should decrease the reaction barrier to C_α -H cleavage. The stabilizing effect would be greater for the π -mechanism because in this case the side chain is in the same plane as the main chain. The effect of the side chain on the reaction barriers is shown for the π -type and σ -type keto-enolic rearrangements of $\text{Ala}^{\bullet+}$. Indeed, both mechanisms are similar to those for $\text{Gly}^{\bullet+}$ (Figure S2 in the Supporting Information), with lower reaction barriers and smaller energy gaps between the two profiles. The TS- σ transition state is 1.0 and 1.4 kcal/mol lower than the TS1- π and 4.5 and 4.9 kcal/mol lower than the TS2- π transition state, as predicted with the B3LYP/6-31+G(d) and B3LYP/6-311++G(d,p) methods, respectively. The CH_3 group has the greatest effect on the TS1- π transition state, making 1,2- and 1,3-shifts nearly degenerate. The stabilizing effect of the side chain is fading at the remote second reaction step; thus, for $\text{Ala}^{\bullet+}$, the TS2- π transition state is notably higher in energy than TS- σ . The CH_3 group also decreases the gap between the σ -type 1,3-shift and the π -type $\text{C}_\alpha \rightarrow \text{NH}_2$ shift from 7.8 kcal/mol for $\text{Gly}^{\bullet+}$ to 3.6 kcal/mol for $\text{Ala}^{\bullet+}$ (Table S1).

In summary, for both $\text{Gly}^{\bullet+}$ and $\text{Ala}^{\bullet+}$, and probably for all RCAAs, the σ -type concerted H-transfer from the C_α to the carboxylic group is energetically more favorable than the stepwise keto-enolic rearrangements.

4. Aromatic Amino Acids: $\text{Trp}^{\bullet+}$, $\text{Tyr}^{\bullet+}$, and $\text{Phe}^{\bullet+}$. (a) $\text{Trp}^{\bullet+}$. Trp contains indole in the side chain and, apparently, has the lowest IE among amino acids⁵ (IE of 3-methylindole is 7.51 eV).³³ Thus, mechanistically, ionization of a neutral gaseous Trp should occur from the aromatic condensed rings. Selected geometries and relative enthalpies of the $\text{Trp}^{\bullet+}$ -keto1, $\text{Trp}^{\bullet+}$ -keto3, $\text{Trp}^{\bullet+}$ -enolic, and $\text{Trp}^{\bullet+}$ -zw1 isomers predicted with the B3LYP/6-31+G(d) method are reported in Figure 6. In contrast to the aliphatic amino acids considered in the present work, the keto1 form of $\text{Trp}^{\bullet+}$ is the lowest-energy isomer. The geometry of $\text{Trp}^{\bullet+}$ -keto1 is very close to that of neutral Trp at the same conformation (reported in the Supporting Information); an unpaired electron and a hole are delocalized among the condensed aromatic rings. The $\text{Trp}^{\bullet+}$ -enolic isomer, with a proton transferred from the C_α to the carboxylic group exhibits an alternative way for delocalization of an unpaired electron along the main chain. This captodative delocalization appears to be less efficient: $\text{Trp}^{\bullet+}$ -enolic is higher in energy than $\text{Trp}^{\bullet+}$ -keto1 by 6.8 kcal/mol. The enolic form has typical covalent bond lengths and a shortened C_α - $\text{C}_{\text{carboxyl}}$ bond (1.407 Å), similar to the enolic forms of the aliphatic amino acids.

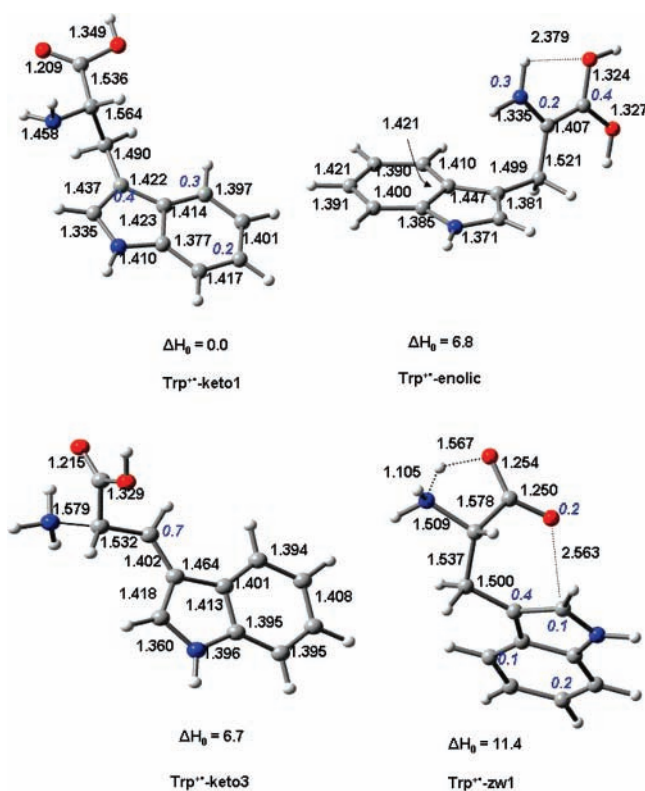


Figure 6. Selected geometries, in Å, and relative enthalpies at 0 K, in kcal/mol, predicted for the lowest-energy conformers of major isomers of $\text{Trp}^{\bullet+}$ with the B3LYP/6-31+G(d) method. Mulliken spin densities are in blue italics.

$\text{Trp}^{\bullet+}$ -zw1 is reminiscent of the keto1 form, which contains a N-H...O hydrogen bond. Mulliken spin densities indicate that an unpaired electron resides essentially on the indole (0.8e) and partly on the carbonyl oxygen, which is involved in the 3e-2c weak bonding with the carbon atom of indole. That is in sharp contrast to the spin localization at the carboxylate group in the zw1 forms of the aliphatic amino acids. The O atom involved in the N-H...O interaction in $\text{Trp}^{\bullet+}$ -zw1 has a zero Mulliken spin density. Thus, the N-H bond is strongly polarized: the N-H distance is 1.105 Å (1.031 and 1.065 Å for $\text{Ser}^{\bullet+}$ -zw1 and $\text{Cys}^{\bullet+}$ -zw1, respectively). All three stabilizing factors, delocalization of an unpaired electron, 3e-2c interaction, and hydrogen bonding, place $\text{Trp}^{\bullet+}$ -zw1 only 11.4 kcal/mol above the lowest-energy $\text{Trp}^{\bullet+}$ -keto1 isomer.

The presence of an aromatic system in the side chain of Trp (and other aromatic amino acids) provides an exceptional mobility of a C_β hydrogen;⁵ this phenomenon is not observed in the aliphatic amino acids. Several low-energy pathways for the migrations of the C_β hydrogen for $\text{TrpGly}^{\bullet+}$ and $\text{GlyTrp}^{\bullet+}$ dipeptides have been previously reported.⁵ H-transfer from the C_β to the amino group yields the $\text{Trp}^{\bullet+}$ -keto3 isomer, which is nearly isoenergetic to the enolic form. For $\text{Trp}^{\bullet+}$ -keto3, an unpaired electron resides essentially on the C_β (0.7) and is stabilized with the adjacent aromatic indole. The N-C bond is elongated (1.579 Å); thus, the loss of NH_3 from $\text{Trp}^{\bullet+}$ -keto3 should be a low-energy process.

Mechanistically, ionization of a neutral gaseous Trp occurs from the aromatic system. The delocalization of an unpaired electron over indole rings is more efficient than the delocalization along the main chain of the captodative enolic form.

(b) $\text{Tyr}^{\bullet+}$. Tyr contains cresol as the side chain and exhibits nearly the same efficacy in forming radical cations as Trp in mass-spectrometry experiments.⁵ Tyr, apparently, has a higher

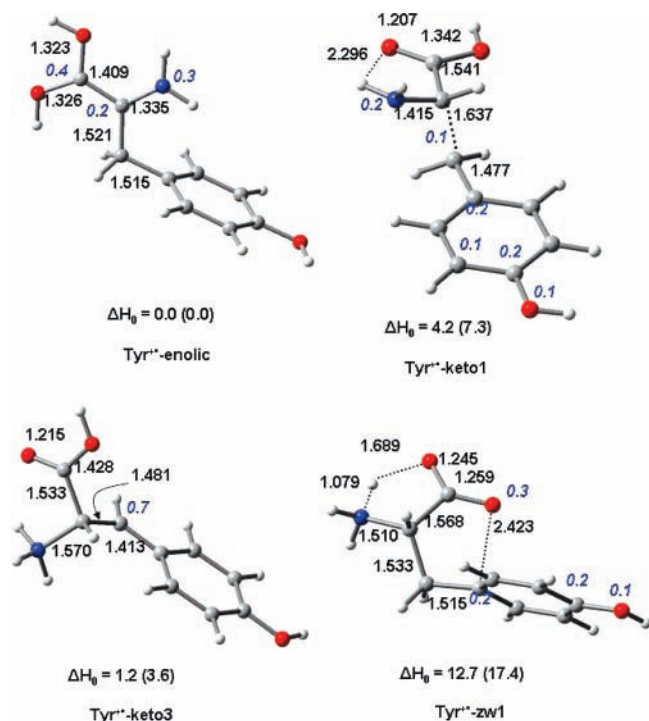


Figure 7. Selected geometries, in Å, and relative enthalpies at 0 K, in kcal/mol, predicted for the lowest-energy conformers of major isomers of Tyr^{*+} using the B3LYP/6-31+G(d) and B3LYP/6-311++G(d,p) (values in parentheses) methods. Mulliken spin densities are in blue italics.

IE than Trp (IE = 8.34 eV for *p*-cresol versus 7.51 eV for 3-methylindole³³). Thus, mechanistically, ionization from the aromatic system might be less favorable than in the case of Trp. Selected geometries and relative enthalpies of the Tyr^{*+} -keto1, Tyr^{*+} -keto3, Tyr^{*+} -enolic, and Tyr^{*+} -zw1 isomers predicted with the B3LYP/6-31+G(d) method are reported in Figure 7. The B3LYP method shows that, indeed, the Tyr^{*+} -keto1 isomer is not the global minimum on the PES. The isomer has an elongated C_α - C_β bond of 1.637 Å. Thus, mechanistically, ionization occurs from the C-C covalent bond rather than from the aromatic ring of Tyr, in contrast to Trp. The Tyr^{*+} -keto3 isomer, which is formed by migration of the C_β hydrogen to the amino group, exhibits the same features as Trp^{*+} -keto3: the N-C bond is elongated (1.570 Å) and an unpaired electron resides on the C_β , stabilized by the adjacent aromatic ring. This isomer is 3.0 and 3.7 kcal/mol lower in energy than the keto1 form of Tyr^{*+} , as predicted with the B3LYP/6-31+G(d) and B3LYP/6-311+G(d,p) methods, respectively.

In contrast to Trp^{*+} , the lowest-energy isomer of Tyr^{*+} is enolic, similar to that of the aliphatic amino acids considered in the present work. However, with the B3LYP/6-31+G(d) method, Tyr^{*+} -enolic is only 1.2 and 4.2 kcal/mol lower in energy than Tyr^{*+} -keto2 and Tyr^{*+} -keto1, respectively. An increase in the basis set to 6-311+G(d,p) increases the gaps to 3.6 and 7.3 kcal/mol, respectively. The zwitterionic isomer, Tyr^{*+} -zw1, has features similar to those of Trp^{*+} -zw1 and similar stabilizing factors: the spin delocalization, the N-H \cdots O hydrogen bond, and the 3e-2c interaction. Thus, Tyr^{*+} -zw1 is only 12.7 and 17.4 kcal/mol higher in energy than the enolic form as predicted with the B3LYP/6-31+G(d) and B3LYP/6-311+G(d,p) methods, respectively.

For Tyr^{*+} , comparable stabilizing effects are achieved by the captodative delocalization of an unpaired electron along the main chain (enolic isomer) and by partial withdrawing of an unpaired

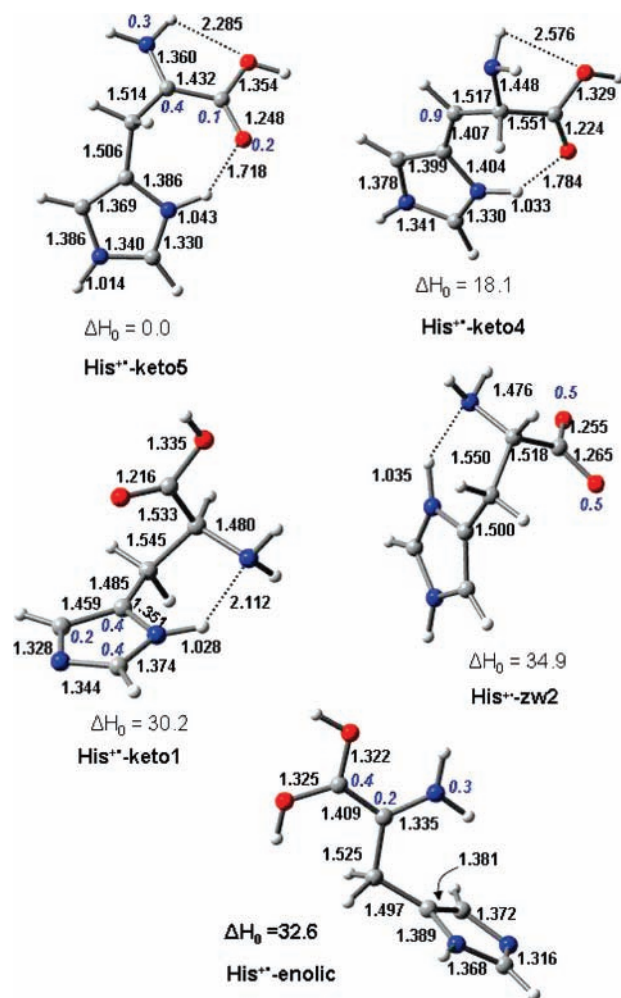


Figure 8. Selected geometries, in Å, and relative enthalpies at 0 K, in kcal/mol, predicted for the lowest-energy conformers of the major isomers of His^{*+} with the B3LYP/6-31+G(d) method. Mulliken spin densities are in blue italics.

electron from C_β to the adjacent ring (keto3); the former stabilizing factor is preferable.

(c) Phe^{*+} . Phenylalanine contains toluene as a side chain. The IE of toluene is 8.8 eV,³³ which is 0.5 and 1.3 eV greater than the IEs of the side chains of Tyr and Trp, respectively. Therefore, one can anticipate Phe^{*+} -enolic to be the lowest-energy isomer. Selected geometries and relative enthalpies of Phe^{*+} -keto1, Phe^{*+} -keto3, Phe^{*+} -enolic, and Phe^{*+} -zw1 predicted with the B3LYP/6-31+G(d) and B3LYP/6-311+G(d,p) methods are reported in the Supporting Information (Figure S3). The geometries, the atomic spin densities, and the ordering of the isomers are similar to those for Tyr^{*+} , with greater energy gaps between the enolic form and the higher-energy isomers.

5. Basic Amino Acids: His^{*+} . His is unique as it contains the aromatic imidazole ring, which is also a strong base. The IE of imidazole is 8.8 eV,³³ similar to that of toluene. The gas-phase proton affinity (PA) of His, along with glutamine, is ca. 230 kcal/mol.³⁴ This is close to the PAs of arginine (249 kcal/mol) and lysine (235 kcal/mol),³⁴ the most basic amino acids. The high PA of His implies that protonation of the imidazole ring in His^{*+} should be a strong stabilizing factor. Therefore, H-transfer should occur to imidazole from either the C_β or C_α . The former transfer results in the formation of a keto4 isomer, with an unpaired electron residing on the C_β , stabilized by the adjacent protonated imidazole. The latter results in the captodative keto5 isomer, with spin delocalized on the N-C α =O

moiety. The H-transfer from the carboxylic group results in the zw2 isomer, with no efficient stabilization of an unpaired electron. Other low-energy forms, His^{•+}-enolic and His^{•+}-keto1, should provide an efficient delocalization of the unpaired electron along the main chain and the aromatic ring, respectively. However, for these isomers, the basic imidazole ring is not protonated, which might not be energetically favorable.

Selected geometries and relative enthalpies of the His^{•+}-keto1, His^{•+}-keto4, His^{•+}-keto5, His^{•+}-enolic, and His^{•+}-zw2 isomers predicted with the B3LYP/6-31+G(d) method are reported in Figure 8. The global-minimum isomer, His^{•+}-keto5, is 18.1 kcal/mol below the nearest-energy isomer, His^{•+}-keto4. Both isomers contain protonated imidazole and two N—H···O hydrogen bonds. Therefore, the energy gap of 18.1 kcal/mol is due to more efficient captodative stabilization compared to the stabilization of an unpaired electron on the C_β by the adjacent protonated imidazole.

Another two isomers, His^{•+}-keto1 and His^{•+}-enolic, with delocalized spin and nonprotonated imidazole, are significantly higher in energy than the lowest keto5 form, by 30.2 and 32.6 kcal/mol, respectively. This difference in energy could be attributed to the protonation of the imidazole ring. A small energetic preference of the keto1 form of 2.4 kcal/mol might be due to the N—H···N hydrogen bonding. The His^{•+}-zw2 isomer represents the structure with protonated imidazole and unpaired electron localized on the carboxylate group. This isomer is above the lowest-energy keto5 isomer by 34.9 kcal/mol. The relative energetics of the five isomers of His^{•+} show that the protonation of imidazole stabilizes the system by ca. 30 kcal/mol; spin delocalization causes a similar decrease in energy.

Conclusions

For RCAAAs, the following stabilizing factors should be considered: delocalization of an unpaired electron, protonation of the basic side chain, hydrogen bonding, and 3e–2c interactions (for sulfur-containing amino acids). The first two factors are the most important. There are three major forms of RCAAAs based on the structure of the carboxylic group: keto (COOH), enolic (C(OH)OH), and zwitterionic (COO[–]).

Spin delocalization is energetically favorable for all the RCAAAs considered in this paper: aliphatic Gly^{•+}, Ala^{•+}, Pro^{•+}, and Ser^{•+}; sulfur-containing Cys^{•+}; aromatic Trp^{•+}, Tyr^{•+}, and Phe^{•+}; and basic His^{•+}. The same results were seen in the previous work on Gly.^{16a} To date, the only amino acid that does not favor spin delocalization is Met^{•+}. It has been previously shown^{13a} that the lowest-energy isomer of Met^{•+} has its spin localized on the sulfur atom of the side chain.

An efficient spin delocalization occurs in the enolic (C(OH)OH) form, with the hydrogen being transferred from C_α to the carboxylic group. An unpaired electron is delocalized along the main chain providing captodative stabilization. The lowest-energy isomers of Gly^{•+},^{16a} Ala^{•+}, Pro^{•+}, Ser^{•+}, Cys^{•+}, Tyr^{•+}, and Phe^{•+} are enolic. For these RCAAAs, the C_α hydrogen acts as an acid and the carboxylic group acts as a base. The enolic structure is probably a lowest-energy isomer for all other aliphatic RCAAAs, which are not basic.

The lowest-energy isomer of His^{•+} is formed upon H-transfer from C_α to the basic imidazole ring rather than to the carboxylic group; that results in a keto form, with an unpaired electron delocalized over the N—C_α=O moiety. One might speculate that the lowest-energy isomers of the radical-cationic basic arginine, lysine, and glutamine have a keto structure similar to that for His^{•+}.

Trp^{•+} has the lowest IE among the aromatic amino acids, and this is the only RCAA that favors its spin delocalized over the aromatic side chain. Thus, the lowest-energy isomer of Trp^{•+} has a keto form, and the same conformation and nearly the same geometry as a neutral gaseous Trp, with no H-transfer. The enolic form of Trp^{•+} is 6.8 kcal/mol higher in energy than the keto form, as predicted using the B3LYP/6-31+G(d) method.

The H-transfer from the C_α to the carboxylic group to yield the enolic form occurs via a concerted mechanism as a σ-type 1,3-shift in the H—C_α—C=O plane. The stepwise mechanisms are somewhat higher in energy for Gly^{•+} and Ala^{•+} and, probably, for all RCAAAs.

The zwitterionic isomers of RCAAAs are high-energy local minima, with spin localized on the carboxylate group (on the carbonyl oxygen and sulfur for Cys^{•+}), that is not energetically favorable. The energy gaps between the enolic and zwitterionic forms are in the range of 22–33 kcal/mol. The exceptions are aromatic Trp^{•+}, Tyr^{•+}, and Phe^{•+}. For these RCAAAs, the zwitterionic isomers have spin delocalized over the aromatic side chains that drops the enolic–zwitterionic gaps below 20 kcal/mol.

Acknowledgment. The financial support of the Natural Science and Engineering Research Council (NSERC) is gratefully acknowledged. P.C.M. thanks the NSERC and University of St. Francis Xavier for Research at St. Francis Xavier University for undergraduate student research awards.

Supporting Information Available: Electronic energies, ZPVE-corrected energies, and Cartesian coordinates for all structures reported and basis sets employed in the form of the Gaussian 03 archive files; potential energy profiles for the H-transfer mechanisms for the Ala^{•+}-keto1 to Ala^{•+}-enolic rearrangement; selected geometries and relative enthalpies for the lowest-energy isomers of Phe^{•+}. This material is available free of charge via the Internet at <http://pubs.acs.org>.

References and Notes

- Chu, I. K.; Rodriguez, C. F.; Lau, T.-C.; Hopkinson, A. C.; Siu, K. W. M. *J. Phys. Chem. B* **2000**, *104*, 3393.
- Chu, I. K.; Rodriguez, C. F.; Hopkinson, A. C.; Siu, K. W. M.; Lau, T.-C. *J. Am. Soc. Mass Spectrom.* **2001**, *12*, 1114.
- Wee, S.; O'Hair, R. A. J.; McFadyen, W. D. *Rapid Commun. Mass Spectrom.* **2002**, *16*, 884.
- Chu, I. K.; Siu, S. O.; Lam, C. N. W.; Chan, J. C. Y.; Rodriguez, C. F. *Rapid Commun. Mass Spectrom.* **2004**, *18*, 1798.
- Bagheri-Majidi, E.; Ke, Y.; Orlova, G.; Chu, I. K.; Hopkinson, A. C.; Siu, K. W. M. *J. Phys. Chem. B* **2004**, *108*, 11170.
- Barlow, C. K.; Wee, S.; McFadyen, W. D.; O'Hair, R. A. J. *Dalton Trans.* **2004**, 3199.
- Chu, I. K.; Lam, C. N. W.; Siu, S. O. *J. Am. Soc. Mass Spectrom.* **2005**, *16*, 763.
- Wee, S.; O'Hair, R. A. J.; McFadyen, W. D. *Int. J. Mass Spectrom.* **2004**, *234*, 101.
- Wee, S.; White, J. M.; McFadyen, W. D.; O'Hair, R. A. J. *Aust. J. Chem.* **2003**, *56*, 1201.
- Barlow, C. K.; McFadyen, W. D.; O'Hair, R. A. J. *J. Am. Chem. Soc.* **2005**, *127*, 6109.
- Lam, C. N. W.; Sou, S. O.; Orlova, G.; Chu, I. K. *Rapid Commun. Mass Spectrom.* **2006**, *20*, 1–7.
- Barlow, C. K.; Moran, D.; Radom, L.; McFadyen, W. D.; O'Hair, R. A. J. *J. Phys. Chem. A* **2006**, *110*, 8304.
- (a) Brunelle, P.; Rauk, A. *J. Phys. Chem. A* **2004**, *108*, 11032. (b) Rickard, G. A.; Gómez-Balderas, R.; Brunelle, P.; Raffa, D. F.; Rauk, A. *J. Phys. Chem. A* **2005**, *109*, 8361. (c) Gómez-Balderas, R.; Raffa, D. F.; Rickard, G. A.; Brunelle, P.; Rauk, A. *J. Phys. Chem. A* **2005**, *109*, 5498. (d) Shustov, G. V.; Spinney, R.; Rauk, A. *J. Am. Chem. Soc.* **2000**, *122*, 1191. (e) Rauk, A.; Armstrong, D. A. *J. Am. Chem. Soc.* **2000**, *122*, 4185. (f) Rauk, A.; Armstrong, D. A.; Fairlie, D. P. *J. Am. Chem. Soc.* **2000**, *122*, 9761.

- (14) (a) Blagojevic, V.; Petrie, S.; Bohme, D. K. *Mon. Not. R. Astron. Soc.* **2003**, 339, L7. (b) Orlova, G.; Blagojevic, V.; Bohme, D. K. *J. Phys. Chem. A* **2006**, 110, 8266.
- (15) Gutowski, M.; Skurski, P.; Simons, J. *J. Am. Chem. Soc.* **2000**, 122, 10159.
- (16) (a) Simon, S.; Sodupe, M.; Bertran, J. *J. Phys. Chem. A* **2002**, 106, 5697. (b) Gil, A.; Bertran, J.; Sodupe, M. *J. Am. Chem. Soc.* **2003**, 125, 7461. (c) Georgieva, I.; Trendafilova, N.; Rodríguez-Santiago, L.; Sodupe, M. *J. Phys. Chem. A* **2005**, 109, 5668. (d) Bertran, J.; Rodríguez-Santiago, L.; Sodupe, M. *J. Phys. Chem. A* **1999**, 103, 2310. (e) Simon, S.; Gil, A.; Sodupe, M.; Bertran, J. *J. Mol. Struct. (THEOCHEM)* **2005**, 727, 191. (f) Rimola, A.; Rodríguez-Santiago, L.; Sodupe, M. *J. Phys. Chem. B* **2006**, 110, 24189. (g) Rodríguez-Santiago, L.; Sodupe, M.; Olivia, A.; Bertran, J. *J. Phys. Chem. A* **2000**, 104, 1256.
- (17) (a) Gray, H. B.; Malmström, B. G.; Williams, R. J. P. *J. Biol. Inorg. Chem.* **2000**, 5, 551. (b) Li, H.; Webb, S. P.; Ivanic, J.; Jensen, J. H. *J. Am. Chem. Soc.* **2004**, 126, 8010. (c) Yanagisawa, S.; Dennison, C. *J. Am. Chem. Soc.* **2005**, 127, 16453.
- (18) Kantorow, M.; Hawse, J. R.; Cowell, T. L.; Benhamed, S.; Pizarro, G. O.; Reddy, V. N.; Hejtmancik, J. F. *Proc. Natl. Acad. Sci. U.S.A.* **2004**, 101, 9654.
- (19) For recent publications see, for example: Hou, L.; Zagorski, M. *J. Am. Chem. Soc.* **2006**, 128, 9260.
- (20) Ehrenfreund, P.; Glavin, D. P.; Botta, O.; Cooper, G.; Bada, J. L. *Proc. Natl. Acad. Sci. U.S.A.* **2001**, 98, 2138.
- (21) Engel, M. H.; Mascko, S. A. *Nature* **1997**, 389, 265.
- (22) Pizzarello, S. *Acc. Chem. Res.* **2006**, 39, 231.
- (23) Frisch, M. J.; Trucks, G. W.; Schlegel, H. B.; Scuseria, G. E.; Robb, M. A.; Cheeseman, J. R.; Montgomery, J. A., Jr.; Vreven, T.; Kudin, K. N.; Burant, J. C.; Millam, J. M.; Iyengar, S. S.; Tomasi, J.; Barone, V.; Mennucci, B.; Cossi, M.; Scalmani, G.; Rega, N.; Petersson, G. A.; Nakatsuji, H.; Hada, M.; Ehara, M.; Toyota, K.; Fukuda, R.; Hasegawa, J.; Ishida, M.; Nakajima, T.; Honda, Y.; Kitao, O.; Nakai, H.; Klene, M.; Li, X.; Knox, J. E.; Hratchian, H. P.; Cross, J. B.; Bakken, V.; Adamo, C.; Jaramillo, J.; Gomperts, R.; Stratmann, R. E.; Yazyev, O.; Austin, A. J.; Cammi, R.; Pomelli, C.; Ochterski, J. W.; Ayala, P. Y.; Morokuma, K.; Voth, G. A.; Salvador, P.; Dannenberg, J. J.; Zakrzewski, V. G.; Dapprich, S.; Daniels, A. D.; Strain, M. C.; Farkas, O.; Malick, D. K.; Rabuck, A. D.; Raghavachari, K.; Foresman, J. B.; Ortiz, J. V.; Cui, Q.; Baboul, A. G.; Clifford, S.; Cioslowski, J.; Stefanov, B. B.; Liu, G.; Liashenko, A.; Piskorz, P.; Komaromi, I.; Martin, R. L.; Fox, D. J.; Keith, T.; Al-Laham, M. A.; Peng, C. Y.; Nanayakkara, A.; Challacombe, M.; Gill, P. M. W.; Johnson, B.; Chen, W.; Wong, M. W.; Gonzalez, C.; Pople, J. A. *Gaussian 03*, revision C.02; Gaussian, Inc.: Wallingford, CT, 2004.
- (24) Becke, A. D. *J. Chem. Phys.* **1993**, 98, 5648.
- (25) Lee, C.; Yang, W.; Parr, R. G. *Phys. Rev. B* **1988**, 37, 785.
- (26) (a) Čizek, J. *Adv. Chem. Phys.* **1969**, 14, 35. (b) Purvis, G. D.; Bartlett, R. J. *J. Chem. Phys.* **1982**, 76, 1910. (c) Scuseria, G. E.; Janssen, C. L.; Schaefer, H. F., III. *J. Chem. Phys.* **1988**, 89, 7382. (d) Scuseria, G. E.; Schaefer, H. F., III. *J. Chem. Phys.* **1989**, 90, 3700. (e) Pople, J. A.; Head-Gordon, M.; Raghavachari, K. *J. Chem. Phys.* **1987**, 87, 5968.
- (27) Gonzalez, C.; Schlegel, H. B. *J. Chem. Phys.* **1989**, 90, 3154.
- (28) Gonzalez, C.; Schlegel, H. B. *J. Phys. Chem.* **1990**, 94, 5523.
- (29) Dennington, R., II; Keith, T.; Millam, J.; Eppinnett, K.; Hovell, W. L.; Gilliland, R. *GaussView*, version 3.09; Semicem, Inc.: Shawnee Mission, KS, 2003.
- (30) *Spartan06*; Wavefunction, Inc.: Irvine, CA.
- (31) (a) Leroy, G.; Sana, M.; Wilante, C. *J. Mol. Struct.* **1991**, 228, 37. (b) Rauk, A.; Yu, D.; Taylor, J.; Shustov, G. V.; Block, D. A.; Armstrong, D. A. *Biochemistry* **1999**, 38, 9089. (c) Yates, B. F.; Bouma, W. J.; Radom, L. *J. Am. Chem. Soc.* **1984**, 106, 5805.
- (32) Espinosa, E.; Molins, E.; Lecomte, C. *Chem. Phys. Lett.* **1998**, 285, 170.
- (33) *NIST chemistry webbook*; <http://webbook.nist.gov/chemistry/>.
- (34) Marksić, Z. B.; Kovačević, B. *Chem. Phys. Lett.* **1999**, 307, 497.